Microstructural Analysis of Shearband Boudin – Preliminary Results

Benedito C. Rodrigues*[1], Mark Peternell[2], António Moura[1], Jorge Pamplona[3]
[1] Centro de Geologia da Universidade do Porto, Rua do Campo Alegre, 687, 4169-007 Porto, Portugal, bjc.rodrigues@gmail.com
[2] Tektonophysik, Johannes-Gutenberg Universität Mainz, 55099 Mainz, Germany
[3] Centro de Investigação Geológica, Ordenamento e Valorização de Recursos, Universidade do Minho, Campus de Gualtar, 4710-057 Braga, Portugal

1. Introduction

The internal structure of a shearband boudin resulting from an original igneous, hydrothermal or metamorphic segregation tabular rigid body is a subject of scientific interest. It allows understanding the deformation mechanisms acting on homogeneous quartz aggregate activated during simple shear progressive deformation.

This communication is focused on the characterization of two main structural aspects: (i) the existence of different internal domains in shearband boudins; (ii) the development of internal structures related with its genesis and evolution, namely, secondary shear planes c' type-I and c' type-II, parameter B-t (mass accumulation sector on blunt tip of shearband boudin) and S-t (sharp tip of shearband boudin) (Pamplona & Rodrigues, 2011a, Pamplona and Rodrigues, 2011b), internal migration of mass (rotation and translation) and mechanisms of ductile deformation activated on the process.

2. Methodology

The obtained results come fundamentally from inputs of five methodologies: (i) Quartz microtextural analysis (classical optical microscopy appointing to the identification to textural features related with internal quartz domains and internal shearband boudin microstructures; (ii) Quartz *c*-axis preferred orientation measurements by the use of an automated fabric analyzer system (Wilson et al., 2007; Peternell et al., 2009; 2010); (iii) Quantification of quartz microstructures by the use of the PolyLx toolbox (Lexa, 2003); (iv) Fractal geometry based analysis of quartz grains to distinguish different quartz populations that developed during formation of the shearband boudin and, (v) Identification of fluid inclusion types, fluid volume density, fluid composition and density, probable isochoric path and consequent temperature and pressure of fluid entrapment, on core older quartz, intercrystalline domains and on the recrystallized quartz.

The Fabric Analyser instrument G50-RGB is an automated and very fast polarizing optical microscope that determines the orientation of *c*-axes of uniaxial crystals at each pixel in the field of view with 2.8 µm/pixel resolution (e.g. Wilson et al., 2007; Peternell et al., 2009; 2010). The output of the instrument is a set of data images and a pixel data file. *c*-axis trend and plunge, retardation (highest birefringence color), orientation, grain boundary and quality images are produced in addition to the conventional crossed polar images.

PolyLx is a Matlab toolbox for structural and microstructural analysis in rocks such as grain size and grain size distribution analysis, grain/grain boundary orientation, strain analysis and many more. The input file has to be a shapefile that contains the objects of interest (e.g. grains, clasts or voids).

By the use of the box-counting method area and perimeter of single crystals are determined on different scales and plotted in a log-log diagram. In case of crystals the data points show a clear linear correlation and the slope of the best fit determines the fractal area-perimeter dimension. A colour coded map of the whole boudin is presented regarding the variation of fractal area-perimeter dimensions.

Fluid inclusion studies. The study of the fluid inclusion population on the old core quartz, on the intercrystalline spaces and inside recrystallized quartz coupled with the metamorphic information of the region, will permit to envisage the PTVX characteristics of the boudin geological history.

3. Results and discussion

Quartz SPOs and CPOs inside the boudin can be grouped into several textural domains. Within the "internal" domains (Fig. 1) *c*-axis orientations are concentrated along a single girdle structure, whereas patterns from the "blunt tip" domains form symmetric and slightly asymmetric cross girdles. Unusually, the single girdle is asymmetric oriented in a low angle to strain X as well as the cross girdle open over strain X and not strain Z.

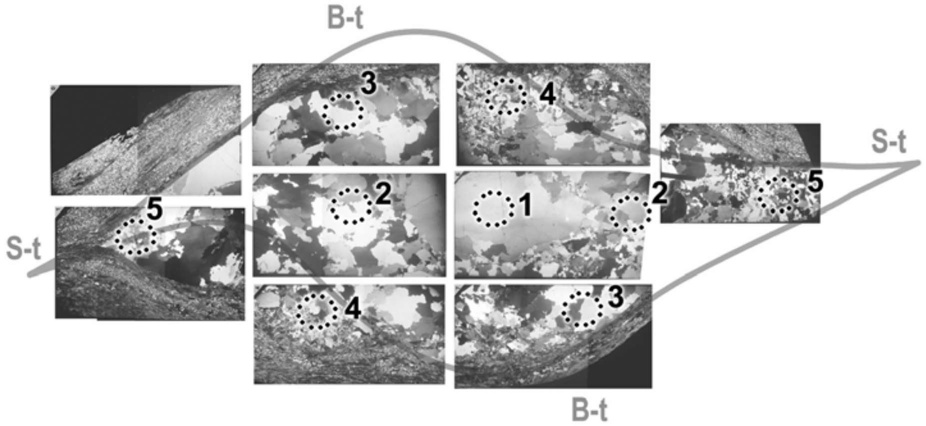

Figure 1 – Dominial analysis of internal structure of shearband boudin. 1- nucleus domain, 2- inner domains, 3- blunt-tip domain, 4- heterogeneous domain, 5- sharp-tip domain.

This indicates that the domains exhibit a rotational increment during boudin formation in relation to the external simple shear regime of 90°. Quartz SPOs from these domains are approx. parallel to the related CPOs indicating that grain boundary and *c*-axis formation occurred in an early stage of boudin formation followed by domain rotation and minor grain boundary migration.

Structurally different domains are present at the boudin's sharp tips. The quartz is finer grained with SPO in a high angle to the CPO and the quartz pattern form a strongly asymmetric cross girdle with a strong maximum parallel strain X. The *c*-axis orientations again indicate a rotational component of the domain with different vorticity to the other domains.

The mapping of fractal area-perimeter dimensions indicates two quartz "populations" with coarser grained quartz in the "internal" and "blunt tip" domains. Along the grain boundaries and the internal "surfaces" (corresponding to c' types) and second quartz "population" formed that is also dominant at the "sharp tip" domains.

The results from the microstructural quantification indicate that the microstructures are different depending on their location inside the boudin but can be assigned to several domains. Quartz microstructures of "internal" and "blunt tip" domains are once they are formed only show rotational component with minor grain boundary migration possibly related to slip on the internal "surfaces" and the "external" simple shear regime. Microstructural change, i.e. recrystallization, occurs along the internal "surfaces" and in the "sharp tip" domains possibly because of strain localization.

The textural domain corresponding to a possible original grain (nucleus domain) is defined by a large quartz crystal exhibiting a losangic pattern of sub-grain boundaries with dominance of a set sub-parallel to <c>. This direction materializes the internal c' type-I. The transition from this domain to the involving ones is made by a rational boundary "jigsaw type" and by muscovite alignments parallel to c' type-I.

B-t and S-t domains are opposite geometric tips on the boudin and also show contrasting textural features: S-t is characterized by a high frequency of regular boundaries with triple junctions delimiting small grains quartz without or slightly undulant extinction. Otherwise, B-t has coarser grains, with a certain amount of internal deformation registered on undulant extinction of quartz grains and a high boundary mobility with intergranular junctions fringed by neo and leftover grains.

The shearband boudin develops two heterogeneous domains were an additional paragenesis occurs formed by Qtz+And+Tur+Ms+Bt. The muscovite is typically hydrothermal (coarser flakes forming fans) and the andaluzite appears as coarse euhedrical grains with pleochroic zoning exhibiting a pink nucleus (Fe-rich) and colorless border.

The fluid inclusion observations, at this stage of the research, only permit to conclude general statements. The distribution of the fluid inclusions population on the older grains (nucleus domain) is heterogeneous; mm^2 scale areas of these grains are avoided of fluids with dimension that permit the observation under the optical microscope (up to 2000 x); also there are areas where it is easy to see groups of 5-20 micra biphasic fluid inclusions of possible primary origin. These are aqueous-rich inclusions with a degree of filling water around 80%. There are also transgranular trails of two fluid types: one with inclusions similar of the previous described (although smaller) and the other filled with small grey-coloured monophasic fluid inclusions possibly carbonic inclusions. Some of these inclusions have a small rim of water (around 10 % volume). Both types of inclusions have negative-shape morphologies which could be a re-equilibration feature instead of a primary characteristic.

4. Conclusions

The multi-approach studies of the internal structure of the shearband boudin identifies that the shearband boudins exhibit different domains (Bt domain, St domain, heterogeneous domain, internal domain and inner surfaces), with distincts mechanical and mineralogical evolutions. Each domain has characteristic that allows to support the deformational history of boudinage process.

The nucleus domain, as a heritage structure of the original tabular body, could be non-rotated during the boudinage process. The B-t domains are those were the mass transport phenomena is more intense and S-t domains those were the recrystallization phenomena is dominant. The heterogeneous domains represent regions were occurs dilatation during the boudinage allowing the migration, into the SiO_2–rich inner boudin body, of alumina-rich fluids and volatiles, which crystallize the typical paragenesis of this domains.

The grain boundary and *c*-axis formation occurred in an early stage of boudin formation followed by domain rotation and minor grain boundary migration

5. References

Drury M, Urai J (1990). Deformation-related recrystallization processes. Tectonophysics, 172: 235-253.

Lexa O (2003). Numerical approaches in structural and microstructural analysis. PhD thesis, Charles University, Prague, Czech Republic.

Moura A (2008). Metallogenesis at the Neves Corvo VHMS deposit (Portugal): a contribution from the study of fluid inclusions. Ore Geology, 34: 354-368.

Pamplona J, Rodrigues BC (2011a). Kinematic interpretation of shearband boudins: New parameters and ratios useful in HT simple shear zones. Journal of Structural Geology, 33: 38-50.

Pamplona J, Rodrigues BC (2011b). Fold boudins: what is that? Geophysical Research Abstracts, Vol. 13, EGU2011-7465.

Peternell M, Hasalová P, Wilson CJL, Piazolo S, Schulmann K (2010). Evaluating quartz crystallographic preferred orientations and the role of deformation partitioning using EBSD and Fabric Analyser techniques. Journal of Structural Geology, 32: 803-817. Doi:10.1016/j.jsg.2010.05.007

Peternell M, Kohlmann F, Wilson CJL, Seiler C, Gleadow AJW (2009). A new approach to crystallographic orientation measurement for apatite fission track analysis: Effects of crystal morphology and implications for automation. Chemical Geology, 265: 527-539. Doi:10.1016/j.chemgeo.2009.05.021

Van Den Kerkhof A, Hein U (2001). Fluid inclusion petrography. Lithos, 55: 27-47.

Wilson CJL, Russell-Head DS, Kunze K, Viola G (2007). The analysis of quartz c-axis fabrics using a modified optical microscope. Journal of Microscopy, 227: 30–41.